An investigation of three-body effects in intermolecular forces. III. Far infrared laser vibration–rotation–tunneling spectroscopy of the lowest internal rotor states of Ar2HCl

ARTICLE *in* THE JOURNAL OF CHEMICAL PHYSICS · MARCH 1993

Impact Factor: 2.95 · DOI: 10.1063/1.464940

3 AUTHORS, INCLUDING:

Richard J Saykally
University of California, Berkeley
460 PUBLICATIONS **28,045** CITATIONS

SEE PROFILE

An investigation of three-body effects in intermolecular forces. III. Far infrared laser vibration–rotation–tunneling spectroscopy of the lowest internal rotor states of Ar_2HCl

M. J. Elrod, J. G. Loeser, and R. J. Saykally
Department of Chemistry, University of California, Berkeley, California 94720

(Received 20 October 1992; accepted 17 December 1992)

The *c*-type intermolecular out-of-plane bend of Ar_2HCl has been observed at 45.2 cm^{-1}, completing the high resolution far infrared measurements of the three lowest-lying Ar_2HCl bending states which correlate to the $j=1$ internal rotational state of the HCl monomer. The rotational and nuclear quadrupole hyperfine structures indicate the existence of a Coriolis perturbation. The perturbing state is postulated to be a heavy-atom stretching overtone that is very nearly degenerate with the out-of-plane bend. A partial reassignment of the previously reported [J. Chem. Phys. **95**, 3182 (1991)] Ar_2HCl in-plane bend is presented and a treatment of Coriolis effects between the in-plane and Σ bends is discussed. Comparison with dynamically rigorous calculations presented in the accompanying paper [J. Chem. Phys. **98**, 5337 (1993)] indicate substantial three-body contributions to the intermolecular potential, which should be determinable from the data presented in this paper.

INTRODUCTION

The investigation of many-body effects in intermolecular interactions has assumed increasing prominence as modern experimental and computational technology has progressed such that it is now possible to begin to address the details of condensed phases of matter. Although the literature of the last several decades is replete with both experimental and theoretical studies of many-body effects, modern *ab initio* calculations have shown that most such work has seriously underestimated the complexity of the problem. For example, Chalasinski and co-workers have undertaken several *ab initio* (supermolecular Møller-Plesset perturbation theory) studies of three- and four-body effects in several van der Waals clusters and have found that the size and form of many-body terms in the potential are strongly system dependent. These calculations have also shown that hydrogen-bonded systems [such as $(H_2O)_3$, $(HF)_3$, $(HCl)_3$, and $(NH_3)_3$] display large three-body effects ($\sim$10% of pairwise contributions) and that these effects are well approximated by a single term in the perturbation expansion.[1,2] Conversely, more weakly bound systems (such as Ar_3, Ar_2H_2O, and Ar_2HCl) are expected to show smaller three-body effects that *cannot* be well approximated by single terms in the perturbation expansion,[3–5] thus potentially making such effects more difficult to determine. Cooper and Hutson[6] have investigated representative models for three-body dispersion, induction, and short-range forces for the Ar_3 system in an effort to determine the effects of these interactions on the molecular energy levels.

The experimental and theoretical techniques presently being used to address many-body forces have been successfully applied to several prototypical binary systems: i.e., ArHCl, ArHF, ArH_2O, and $ArNH_3$.[7–10] Such binary van der Waals complexes have been the subject of intense experimental study by high resolution microwave,[11] far infrared,[12] and near infrared[13] spectroscopy. In particular, the measurement of the low-lying intermolecular vibrations of these complexes has proven to be the most important experimental data, since these motions sample an extensive region of the intermolecular potential energy surface. Therefore, these data, in combination with efficient computational techniques, have permitted the determination of accurate global intermolecular potential surfaces for several of these systems. Although the qualitative details of these surfaces have been firmly established, their quantitative accuracy is critically important for the purpose of the determination of many-body forces, as these effects will be manifested as small deviations from pairwise additivity. Rare-gas dimers clustered with the hydrogen halides are an obvious choice for the study of three-body effects since the rare-gas pair potentials have been well determined by a variety of experimental techniques, and the rare-gas–hydrogen halide systems have been the corresponding prototypes for *anisotropic* pair interactions. Of these systems, the ArHCl potential is one of the most thoroughly characterized. Recently, Hutson,[7] fit all existing microwave, far infrared, and near infrared data for several ArHCl isotopes to a potential that was explicitly dependent on the HCl monomer vibration. The new potential [denoted H6(4,3,0)] certainly represents one of the most accurate existing anisotropic potential energy surfaces, although the most recent far infrared spectroscopic studies have shown that small, yet significant, inaccuracies may exist in the secondary minimum region of the potential.[14]

For the reasons discussed above, recent work concerning the effects of many-body forces in intermolecular forces has largely centered around the Ar_2HX systems,[15–19] with the Ar_2HCl complex receiving the most extensive experimental and theoretical scrutiny. The eventual goal of this work is to measure all spectroscopically accessible states of Ar_2HCl and thus ultimately characterize the full intermolecular potential energy surface, thereby deducing from the form of three-body effects. Towards that end, we have pre-

 0021-9606/93/075352-10$06.00

viously reported the measurement of two intermolecular vibration–rotation bands using far infrared laser spectroscopy.[16–17] These vibrations (and the one reported in the present work) are best understood by considering the HCl subunit as a nearly free rotor. In this case, the lowest-lying intermolecular bending states correlate to the $j=1$ internal rotational state of the HCl monomer. The intermolecular potential serves to split the threefold spatial degeneracy of the HCl $j=1$ rotational state, resulting in three unique bending states. Following the notation of Cooper and Hutson,[20] these states are identified as the Σ bend (by analogy to ArHCl) and the in-plane and out-of-plane bends (which correspond to the two components of the Π bend of ArHCl). In order to prevent any possible confusion, it should be noted that in previously reported work, we have referred to the Σ bend as the parallel bend. In the present work, we report a partial reassignment of the in-plane bend, an estimate of the effect of Coriolis mixing between the in-plane bend and the Σ bend, and the measurement and analysis of the third $j=1$ state, the out-of-plane bend.

EXPERIMENT

The far infrared vibration–rotation–tunneling spectra of Ar_2HCl were observed in a continuous supersonic planar jet expansion probed by a tunable far infrared laser spectrometer. The spectrometer has been described in detail previously[21,22] so only a brief description here will follow. The tunable far infrared radiation is generated by mixing an optically pumped line-tunable far infrared gas laser with continuously tunable frequency modulated microwaves in a Schottky barrier diode to generate light at the sum and difference frequencies ($\nu=\nu_{FIR}\pm\nu_{MW}$). The tunable radiation is separated from the much stronger fixed frequency radiation with a Michelson polarizing interferometer and is then directed to multipass optics which encompass the supersonic expansion. After passing ~ 10 times through the expansion, the radiation is detected by a liquid helium cooled Putley-mode InSb detector and the signal is demodulated at $2f$ by a lock-in amplifier. $Ar_m[HCl]_n$ clusters were produced by continuously expanding a 0.5% HCl in argon mixture at a stagnation pressure of 2 atm through a 10 cm by 25 μm slit nozzle planar jet into a vacuum chamber pumped by a 1200 l/s Roots pump. The following far infrared lasers provided the fixed frequency radiation: 1299.9954 GHz CH_3OD, and 1397.1186 GHz CH_2F_2. The unstabilized far infrared laser is typically characterized by a short-term frequency drift of <100 kHz and a long-term drift of ca. 1 MHz. However, the 1397 GHz CH_2F_2 laser exhibited an unusually large long-term frequency drift (~ 10 MHz) and consequently all absorption features were measured in reference to the $J=1\rightarrow 2$; $F=3/2\rightarrow 1/2$ transition of H ^{35}Cl (1251.480 94 GHz) (Ref. 23) to yield an absolute frequency accuracy of less than 400 kHz for these transitions (absolute frequencies above 1350 GHz). A representative spectrum is presented in Fig. 1.

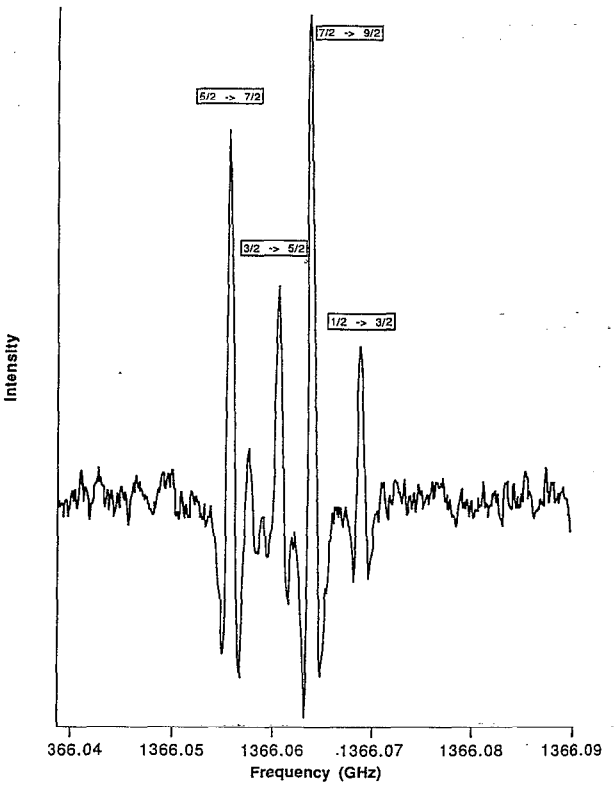

FIG. 1. Experimental trace of the $2_{20}\rightarrow 3_{30}$ transition of the out-of-plane bend of Ar_2H ^{35}Cl. The individual nuclear hyperfine components are labeled by their F quantum numbers.

RESULTS AND ANALYSIS

Equilibrium geometry and nuclear spin statistical weights

The Fourier-transform microwave spectroscopy work of Klots *et al.* established the vibrationally averaged ground state geometry of Ar_2HCl as a planar T-shaped asymmetric top of C_{2v} symmetry.[24,25] Due to the fact that rotation about the C_2 axis involves exchange of identical boson nuclei (^{40}Ar; $I=0$) the total wave function must be symmetric with respect to this motion. Because the C_2 axis corresponds to the a inertial axis in the ground state, nonzero nuclear spin statistical weights exist only for even K_p rotational levels.

Assignment techniques

Because of spectral congestion (typically >400 absorptions/cm^{-1}), varying experimental sensitivity, and the possible existence of perturbations that may destroy ordinarily recognizable features of the spectrum, the task of assigning the observed transitions to their upper and lower state rotational quantum numbers is extremely difficult. We have chosen the common practice of using known ground state energy levels (combination differences) as an assignment technique, while specifically tailoring the details of the method to the characteristics of the experiment and the system under study. As noted in the experiment section, the short-term (several minutes) frequency drift of the unlocked far infrared laser is extremely

small (<100 kHz) and the long-term (day-to-day) drift is substantially larger (usually ~ 1 MHz). Therefore, absorption features separated by less than 100 MHz are characterized by a very high relative frequency accuracy. The individual components of the nuclear quadrupole hyperfine structure associated with each rovibrational transition observed for Ar_2HCl therefore possess a very high internal frequency accuracy. In contrast, the rovibrational line centers are often separated by several thousand MHz and therefore possess a lower relative frequency accuracy. Rotational-hyperfine energy levels of the ground state of Ar_2HCl were calculated from the work of Klots *et al.*[24] and experimental far infrared combination differences were compared to calculated values to obtain an assignment for the far infrared spectrum. Due to the very high spectral density, many coincidental (and incorrect) assignments maybe obtained from rotational combination differences alone. Although increased long-term frequency accuracy (as was obtained by referencing several absorptions to an internal standard for one of the bands) substantially reduces coincidental assignments, the inclusion of the very accurate hyperfine combination differences proved to be crucial in discriminating correct assignments from merely coincidental ones.

Reassignment of the in-plane bend

We previously reported an assignment and the corresponding molecular constants for a vibration (a *b*-type band centered at 37.2 cm^{-1}) we tentatively identified as the in-plane bend.[17] Since that time, Cooper and Hutson[20] have carried out more rigorous dynamical calculations on the spectroscopic properties of Ar_2HCl, and these results suggested that some of the experimental conclusions reached for this state may be in error. The observed transitions for that band were subjected to the more rigorous combination difference method outlined above and it was indeed found that a few of the transitions had been misassigned. The properly assigned hyperfine-free line centers (Table I) were fit to a Watson *S*-reduced Hamiltonian[26] with the ground state constants held fixed at the values previously determined. In cases where particular distortion constants were not determinable from the data, these parameters were fixed to their ground state values. The nuclear quadrupole hyperfine coupling constants (χ_{xx}, χ_{yy}, and χ_{zz}) were determined in a separate least-squares fit, with the line centers determined from the rotational fit. The first-order matrix elements of the nuclear quadrupole Hamiltonian were calculated in the coupled basis set $|JKIF\rangle$ ($F=I+J$; $I=3/2$ for both ^{35}Cl and ^{37}Cl).[27] The upper state coupling constants were fit with the ground state coupling constants held fixed at the values determined by Klots *et al.*[24,25]

The principal effect of the revised assignments on the previously reported molecular constants[17] is that the fitted values determined from the off-diagonal matrix elements (oblate symmetric top basis) in both the rotational and nuclear quadrupole Hamiltonian matrices are changed. Therefore, ν_0, B_x+B_y, B_z, and χ_{zz} are essentially unchanged from the previous analysis while B_x-B_y (and

TABLE I. Observed transitions and residuals (MHz) for in-plane bend.

Transition	$Ar_2H\,^{35}Cl$		$Ar_2H\,^{37}Cl$	
$J'_{K_pK_o}\leftarrow J''_{K_pK_o}$	Frequency	Res.	Frequency	Res.
$1_{10}\leftarrow 2_{21}$	1 109 016.5	−1.0		
$1_{10}\leftarrow 1_{01}$	1 115 952.8	0.6		
$2_{12}\leftarrow 3_{03}$	1 109 071.2	−0.8		
$2_{12}\leftarrow 1_{01}$	1 119 257.4	−1.9		
$3_{12}\leftarrow 4_{23}$	1 105 572.7	0.5		
$3_{12}\leftarrow 3_{03}$	1 119 168.2	−0.9		
$3_{12}\leftarrow 3_{21}$	1 112 513.3	0.8		
$3_{13}\leftarrow 4_{04}$	1 107 278.1	−0.1		
$3_{13}\leftarrow 2_{02}$	1 120 812.0	−1.1		
$3_{30}\leftarrow 3_{21}$	1 115 937.0	0.4		
$3_{30}\leftarrow 2_{21}$	1 125 845.6	−0.1	1 125 131.7	1.0
$3_{31}\leftarrow 2_{20}$	1 124 229.5	−2.4		
$4_{13}\leftarrow 5_{24}$	1 103 747.1	0.3		
$4_{13}\leftarrow 4_{04}$	1 120 741.3	−0.5		
$4_{13}\leftarrow 4_{22}$	1 110 521.2	1.2		
$4_{13}\leftarrow 3_{22}$	1 124 068.3	−0.7		
$4_{14}\leftarrow 5_{05}$	1 105 449.9	−0.6	1 105 196.4	0.3
$4_{14}\leftarrow 4_{23}$	1 108 763.7	0.3		
$4_{14}\leftarrow 3_{03}$	1 122 359.7	−0.5	1 121 786.7	0.7
$4_{31}\leftarrow 4_{22}$	1 117 363.6	2.9		
$4_{31}\leftarrow 4_{40}$	1 113 831.9	3.0		
$4_{32}\leftarrow 4_{23}$	1 119 035.4	−0.3		
$4_{32}\leftarrow 3_{21}$	1 125 975.2	−0.9		
$5_{14}\leftarrow 5_{23}$			1 108 340.6	0.5
$5_{14}\leftarrow 4_{23}$	1 125 592.0	−1.2	1 124 968.5	0.1
$5_{15}\leftarrow 6_{06}$	1 103 589.1	−0.5		
$5_{15}\leftarrow 4_{04}$	1 123 874.6	−0.8	1 123 274.0	−0.4
$5_{33}\leftarrow 5_{24}$	1 120 574.5	0.8	1 120 044.8	−0.8
$5_{33}\leftarrow 5_{42}$	1 110 284.2	0.5	1 109 867.2	0.2
$5_{33}\leftarrow 4_{22}$	1 127 346.9	0.0	1 126 796.1	0.7
$5_{50}\leftarrow 6_{61}$	1 094 298.3	0.6		
$5_{50}\leftarrow 5_{41}$	1 115 892.2	1.5		
$5_{50}\leftarrow 4_{41}$	1 132 086.6	0.8	1 131 113.4	1.0
$5_{51}\leftarrow 5_{42}$	1 117 132.2	−0.4		
$5_{51}\leftarrow 4_{40}$	1 130 662.6	−1.4	1 130 268.0	−0.8
$6_{15}\leftarrow 5_{24}$	1 127 076.5	−0.6	1 126 429.0	−0.8
$6_{16}\leftarrow 5_{05}$	1 125 357.3	−0.5	1 124 730.2	−1.1
$6_{33}\leftarrow 7_{44}$	1 096 607.4	0.1		
$6_{33}\leftarrow 6_{24}$	1 120 377.6	0.1		
$6_{33}\leftarrow 6_{42}$	1 110 313.1	1.4		
$6_{33}\leftarrow 5_{42}$			1 129 663.9	0.0
$6_{34}\leftarrow 6_{25}$	1 122 080.6	0.8		
$6_{34}\leftarrow 6_{43}$	1 108 419.7	0.6	1 108 152.8	1.1
$6_{34}\leftarrow 5_{23}$	1 128 800.5	0.3		
$6_{51}\leftarrow 6_{42}$	1 117 145.1	3.1	1 116 560.4	1.2
$6_{51}\leftarrow 6_{60}$			1 111 670.6	1.2
$6_{52}\leftarrow 6_{43}$	1 118 683.6	−1.4		
$7_{16}\leftarrow 8_{27}$	1 098 074.3	−0.8	1 097 979.8	−0.7
$7_{16}\leftarrow 7_{07}$	1 125 259.3	−0.9		
$7_{16}\leftarrow 6_{25}$	1 128 528.9	−0.3	1 127 858.2	−0.1
$7_{17}\leftarrow 6_{06}$	1 126 807.9	−0.5	1 126 155.8	−1.5
$7_{34}\leftarrow 8_{45}$	1 094 689.0	0.0	1 094 695.4	−0.2
$7_{34}\leftarrow 7_{25}$	1 121 852.8	1.0		
$7_{34}\leftarrow 7_{43}$	1 108 239.1	0.8	1 108 159.6	−0.1
$7_{34}\leftarrow 6_{43}$	1 131 971.6	0.2	1 131 259.1	−0.3
$7_{35}\leftarrow 8_{26}$	1 096 380.1	0.0		
$7_{35}\leftarrow 6_{24}$	1 130 248.8	−1.1	1 129 566.8	0.0
$7_{52}\leftarrow 6_{61}$	1 134 597.4	−0.6		
$7_{53}\leftarrow 7_{44}$	1 120 155.5	0.0	1 119 675.2	0.1
$7_{53}\leftarrow 6_{42}$	1 133 860.3	0.4		
$7_{71}\leftarrow 6_{60}$	1 136 817.7	1.3	1 136 339.2	2.1
$8_{17}\leftarrow 9_{28}$	1 096 123.8	−0.2	1 096 070.2	−0.1
$8_{17}\leftarrow 8_{08}$	1 126 702.3	−1.5		
$8_{17}\leftarrow 7_{26}$	1 129 950.1	−1.1	1 129 256.4	−0.8
$8_{18}\leftarrow 9_{09}$	1 097 816.9	−0.2	1 097 717.3	−0.9
$8_{18}\leftarrow 7_{07}$	1 128 228.0	−0.2	1 127 553.0	−0.4
$8_{35}\leftarrow 9_{46}$	1 092 743.0	0.3	1 092 790.0	−1.3
$8_{35}\leftarrow 8_{26}$	1 123 296.5	0.2		
$8_{35}\leftarrow 7_{44}$	1 133 395.6	−0.3	1 132 681.3	−0.1

TABLE I. (*Continued.*)

Transition $J'_{K_pK_o} \leftarrow J''_{K_pK_o}$	Ar_2H ^{35}Cl Frequency	Res.	Ar_2H ^{37}Cl Frequency	Res.
$8_{36} \leftarrow 9_{27}$	1 094 431.4	−0.6		
$8_{36} \leftarrow 8_{27}$	1 124 997.9	−0.7	1 124 403.9	1.4
$8_{36} \leftarrow 7_{25}$	1 131 672.7	0.2	1 130 963.6	−0.8
$8_{53} \leftarrow 8_{44}$	1 119 913.3	−0.1		
$8_{54} \leftarrow 9_{45}$	1 091 059.2	−0.4		
$8_{54} \leftarrow 8_{45}$	1 121 599.9	0.8	1 121 093.1	−1.4
$8_{54} \leftarrow 7_{43}$	1 135 147.8	−0.6		
$8_{71} \leftarrow 8_{62}$	1 116 980.0	−3.0		
$9_{18} \leftarrow 10_{29}$	1 094 144.5	−0.6	1 094 132.3	−0.6
$9_{18} \leftarrow 8_{27}$	1 131 344.5	0.0	1 130 628.4	0.3
$9_{19} \leftarrow 10_{010}$	1 095 834.8	0.8	1 095 775.8	−0.2
$9_{19} \leftarrow 8_{08}$	1 129 618.7	0.0	1 128 920.0	−1.0
$9_{36} \leftarrow 10_{47}$	1 090 769.3	−0.8		
$9_{36} \leftarrow 9_{27}$	1 124 711.4	−0.9		
$9_{36} \leftarrow 8_{45}$	1 134 788.9	−1.1		
$9_{37} \leftarrow 10_{28}$	1 092 456.1	−0.5	1 092 492.6	−0.8
$9_{37} \leftarrow 9_{28}$	1 126 413.0	−1.1		
$9_{37} \leftarrow 8_{26}$	1 133 067.7	0.5	1 132 336.9	0.5
$9_{54} \leftarrow 10_{65}$	1 087 415.4	0.6		
$9_{54} \leftarrow 9_{45}$	1 121 325.6	0.8		
$9_{54} \leftarrow 8_{63}$	1 138 243.6	−0.3		
$9_{55} \leftarrow 10_{46}$	1 089 087.4	−0.6		
$9_{55} \leftarrow 9_{46}$	1 123 015.1	0.3		
$9_{55} \leftarrow 8_{44}$	1 136 520.4	0.0		
$9_{73} \leftarrow 9_{64}$			1 119 257.4	1.1
$9_{91} \leftarrow 10_{82}$			1 086 492.6	−0.7
$10_{19} \leftarrow 11_{210}$	1 092 139.5	−0.5	1 092 169.5	−0.3
$10_{19} \leftarrow 9_{28}$	1 132 711.3	0.7		
$10_{110} \leftarrow 11_{011}$	1 093 825.1	0.9	1 093 808.4	0.6
$10_{110} \leftarrow 9_{09}$	1 130 982.1	0.7	1 130 261.2	−0.5
$10_{37} \leftarrow 11_{48}$	1 088 771.8	−1.0		
$10_{37} \leftarrow 10_{28}$	1 126 100.3	−1.3		
$10_{37} \leftarrow 9_{46}$	1 136 157.8	−0.8	1 135 396.4	−2.5
$10_{38} \leftarrow 11_{29}$	1 090 455.3	−0.5	1 090 534.1	−0.8
$10_{38} \leftarrow 9_{27}$	1 134 434.8	−0.6	1 133 682.1	−0.8
$10_{55} \leftarrow 11_{66}$	1 085 419.7	0.2		
$10_{55} \leftarrow 10_{46}$	1 122 713.2	0.3		
$10_{55} \leftarrow 9_{46}$	1 139 619.6	−0.5		
$10_{56} \leftarrow 9_{45}$	1 137 884.0	−0.6		
$10_{74} \leftarrow 10_{65}$	1 121 032.4	0.0		
$10_{92} \leftarrow 10_{83}$	1 117 611.9	0.4		
$11_{110} \leftarrow 12_{211}$			1 090 182.9	0.0
$11_{111} \leftarrow 12_{012}$	1 091 791.9	2.6	1 091 817.3	2.1
$11_{111} \leftarrow 10_{010}$	1 132 320.6	2.5	1 131 578.2	1.2
$11_{38} \leftarrow 12_{49}$	1 086 752.5	−0.2		
$11_{38} \leftarrow 10_{47}$	1 137 503.3	−0.2		
$11_{39} \leftarrow 12_{210}$	1 088 431.3	−0.2	1 088 552.3	−0.8
$11_{39} \leftarrow 10_{28}$	1 135 779.0	0.0	1 135 004.4	−0.9
$11_{56} \leftarrow 11_{47}$	1 124 077.3	−0.2		
$11_{56} \leftarrow 10_{65}$	1 140 959.4	0.3		
$12_{111} \leftarrow 11_{210}$			1 134 589.3	0.8
$12_{112} \leftarrow 13_{013}$	1 089 730.9	−0.5	1 089 800.8	0.5
$12_{112} \leftarrow 11_{011}$	1 133 631.6	1.0	1 132 871.2	2.4
$12_{310} \leftarrow 13_{211}$	1 086 387.6	1.8		
$12_{310} \leftarrow 12_{49}$			1 096 380.1	−0.2
$12_{310} \leftarrow 11_{29}$	1 137 101.4	1.4		
$12_{57} \leftarrow 12_{48}$	1 125 420.8	0.4		
$12_{57} \leftarrow 11_{66}$	1 142 279.9	0.8		
$13_{112} \leftarrow 14_{213}$			1 086 147.4	1.6
$13_{112} \leftarrow 12_{211}$			1 135 865.1	1.0
$13_{113} \leftarrow 14_{014}$	1 087 652.1	−0.5		
$13_{113} \leftarrow 12_{012}$	1 134 920.4	−0.7	1 134 139.2	0.1
$13_{310} \leftarrow 13_{211}$			1 129 474.6	−0.1
$13_{310} \leftarrow 12_{49}$			1 139 304.8	−0.1
$13_{311} \leftarrow 12_{210}$			1 137 585.8	1.0
$14_{114} \leftarrow 15_{015}$	1 085 554.4	−0.9		
$14_{114} \leftarrow 13_{013}$	1 136 190.7	−0.9	1 135 389.5	−0.7
$15_{115} \leftarrow 14_{014}$	1 137 443.8	−1.5	1 136 621.9	−2.4
$16_{116} \leftarrow 15_{015}$	1 138 686.6	2.3		

TABLE II. Molecular constants (MHz) for in-plane bend (1σ uncertainties).

	Ar_2H ^{35}Cl	Ar_2H ^{37}Cl
ν_0	1 115 098.6(3)	1 114 654.1(5)
B_x	1 683.61(2)	1 683.98(3)
B_y	1 682.42(2)	1 621.21(2)
B_z	826.702(9)	811.215(9)
D_J	0.014 07(13)	0.014 74(19)
D_{JK}	−0.041 8(3)	−0.040 7(4)
D_K	0.022 47(19)	0.020 7(2)
d_1	0.002 479(fixed)	0.002 927(fixed)
d_2	−0.0034(3)	−0.000 456(fixed)
rms error	1.0	1.0

thus the individual values of B_x and B_y) and $\chi_{xx}-\chi_{yy}$ have now been correctly determined. Due to the possibility of rotational axis switching, the molecular constants are expressed in a molecule-fixed axis system as explained in Ref. 17, rather than the conventional principal axis system. The rotational parameters are reported in Table II and the hyperfine coupling constants are reported in Table V for both Ar_2H ^{35}Cl and Ar_2H ^{37}Cl. In order to compare the experimental coupling constants to theoretical values, the following equations provide the relation between these constants and the relevant angular expectation values:

$$\chi_{xx}=\chi_{HCl}\langle P_2(\cos\theta)\rangle, \tag{1}$$

$$\chi_{yy}-\chi_{zz}=\tfrac{3}{2}\chi_{HCl}\langle\Delta(\theta,\phi)\rangle. \tag{2}$$

Here χ_{HCl} is the nuclear quadrupole coupling constant of the uncomplexed HCl monomer and $\langle\Delta(\theta,\phi)\rangle = \sin^2\theta\cos 2\phi$. The deviation of $\langle P_2(\cos\theta)\rangle$ from unity is a measure of the bending amplitude of the HCl monomer, whereas the deviation of $\langle\Delta(\theta,\phi)\rangle$ from zero characterizes the anisotropy of the torsional motion (positive values indicating in-plane localization and negative values indicating out-of-plane localization). The positive sign of the corrected $\langle\Delta(\theta,\phi)\rangle$ value (Table V) indicates that this state is indeed the in-plane bend.

The out-of-plane bend

The out-of-plane bend of Ar_2HCl is characterized by very dense Q-branch structure (indicative of a c-type transition) and was observed around 45.2 cm^{-1}. Due to the values of the upper state nuclear quadrupole coupling constants, it was possible to resolve all four of the strong $\Delta F = \Delta J$ hyperfine components for a large number of the rovibrational transitions. These transitions were assigned according to the method outlined above and are recorded in Table III. Once again hyperfine-free line centers were fitted to a Watson S-reduced Hamiltonian and the nuclear quadrupole structure was separately fitted as previously discussed for the in-plane bend. The results of the rotational fit are contained in Table IV for both the Ar_2H ^{35}Cl and Ar_2H ^{37}Cl isotopes. The results of the nuclear quadrupole hyperfine fit are compiled in Table V.

TABLE III. Observed transitions and residuals (MHz) for out-of-plane bend.

Transition $J'_{K_pK_o} \leftarrow J''_{K_pK_o}$	Ar_2H ^{35}Cl Frequency	Res.	Ar_2H ^{37}Cl Frequency	Res.
$2_{11} \leftarrow 3_{21}$	1 345 392.1	−30.9		
$2_{11} \leftarrow 2_{21}$	1 355 300.5	−31.6		
$2_{11} \leftarrow 1_{01}$	1 362 233.4	−33.5		
$3_{12} \leftarrow 4_{22}$	1 342 111.4	−17.8	1 342 367.3	−24.8
$3_{12} \leftarrow 3_{22}$	1 355 661.6	−16.7		
$3_{12} \leftarrow 2_{02}$	1 365 869.3	−16.5	1 365 568.6	−23.8
$3_{30} \leftarrow 4_{40}$	1 342 205.2	−25.9	1 342 232.4	−14.4
$3_{30} \leftarrow 2_{20}$	1 366 062.1	−24.8	1 365 798.8	−15.8
$3_{31} \leftarrow 4_{41}$	1 341 942.3	−18.6		
$3_{31} \leftarrow 2_{21}$	1 365 987.5	−17.0		
$4_{13} \leftarrow 5_{23}$			1 339 188.2	3.7
$4_{13} \leftarrow 3_{03}$			1 369 151.1	3.3
$4_{14} \leftarrow 5_{24}$	1 338 562.3	0.0		
$4_{14} \leftarrow 4_{04}$	1 355 555.5	−1.8		
$4_{31} \leftarrow 5_{41}$	1 339 651.8	−32.7	1 339 887.9	−6.9
$4_{31} \leftarrow 3_{21}$	1 369 982.0	−32.1	1 369 473.0	−7.0
$4_{32} \leftarrow 5_{42}$	1 339 137.0	−26.3	1 339 303.2	4.7
$4_{32} \leftarrow 4_{22}$	1 356 200.3	−26.2		
$4_{32} \leftarrow 3_{22}$	1 369 749.3	−26.3	1 369 397.2	4.3
$5_{14} \leftarrow 6_{24}$	1 335 797.9	−1.5	1 336 084.6	12.0
$5_{14} \leftarrow 5_{24}$	1 356 180.9	−3.2		
$5_{14} \leftarrow 4_{04}$	1 373 175.9	−3.2	1 372 732.2	11.8
$5_{15} \leftarrow 6_{25}$	1 335 349.8	30.5		
$5_{15} \leftarrow 5_{05}$	1 355 742.7	30.8		
$5_{32} \leftarrow 6_{42}$	1 336.604.3	6.9		
$5_{32} \leftarrow 4_{22}$	1 373 828.6	7.5		
$5_{33} \leftarrow 6_{43}$	1 336 163.3	−8.7	1 336 443.8	23.6
$5_{33} \leftarrow 5_{23}$	1 356 543.9	−9.2	1 356 447.8	24.6
$5_{33} \leftarrow 4_{23}$	1 373 528.9	−9.2	1 373 076.0	24.0
$5_{50} \leftarrow 6_{60}$	1 336 343.8	−14.6		
$5_{50} \leftarrow 4_{40}$	1 373 922.7	−13.5		
$5_{51} \leftarrow 6_{61}$	1 335 972.8	5.1		
$5_{51} \leftarrow 4_{41}$	1 373 759.6	3.8		
$6_{15} \leftarrow 7_{25}$	1 332 693.8	11.0		
$6_{15} \leftarrow 6_{25}$	1 356 471.7	8.7		
$6_{15} \leftarrow 5_{05}$	1 376 864.6	9.0		
$6_{16} \leftarrow 7_{26}$	1 332 195.2	97.8		
$6_{16} \leftarrow 6_{06}$	1 355 984.3	97.5		
$6_{33} \leftarrow 7_{43}$	1 333 686.8	129.5		
$6_{33} \leftarrow 6_{43}$	1 357 421.0	130.6		
$6_{33} \leftarrow 5_{23}$	1 377 801.8	130.3		
$6_{34} \leftarrow 7_{44}$	1 333 038.6	−120.6		
$6_{34} \leftarrow 6_{24}$	1 356 808.7	−120.7		
$6_{34} \leftarrow 5_{24}$	1 377 193.2	−120.9		
$6_{51} \leftarrow 7_{61}$	1 334 415.4	−31.0	1 334 536.4	10.6
$6_{51} \leftarrow 5_{41}$	1 378 254.3	−30.9	1 377 482.3	9.8
$6_{52} \leftarrow 7_{62}$	1 333 638.5	−29.0		
$6_{52} \leftarrow 6_{42}$	1 357 696.5	−30.4		
$6_{52} \leftarrow 5_{42}$	1 377 857.1	−30.3		
$7_{16} \leftarrow 8_{26}$	1 329 618.4	30.2		
$7_{16} \leftarrow 7_{26}$	1 356 791.0	28.6	1 356 648.5	11.8
$7_{16} \leftarrow 6_{06}$	1 380 580.1	28.4	1 379 980.8	11.4
$7_{17} \leftarrow 8_{27}$	1 329 144.4	247.5		
$7_{17} \leftarrow 7_{07}$	1 356 331.0	248.9		
$7_{34} \leftarrow 8_{44}$	1 330 610.7	−30.2		
$7_{34} \leftarrow 6_{24}$	1 381 528.6	−30.0		
$7_{35} \leftarrow 8_{45}$	1 330 155.4	−9.9	1 330 548.1	−1.8

TABLE III. (*Continued.*)

Transition $J'_{K_pK_o} \leftarrow J''_{K_pK_o}$	Ar_2H ^{35}Cl Frequency	Res.	Ar_2H ^{37}Cl Frequency	Res.
$7_{35} \leftarrow 7_{25}$	1 357 317.2	−11.5	1 357 173.4	−0.9
$7_{35} \leftarrow 6_{25}$	1 381 097.0	−11.0	1 380 488.0	−2.1
$7_{52} \leftarrow 8_{62}$	1 331 747.0	58.3		
$7_{52} \leftarrow 7_{62}$	1 358 290.4	58.8		
$7_{52} \leftarrow 6_{42}$	1 382 349.5	58.6		
$7_{53} \leftarrow 8_{63}$	1 331 000.4	−3.7	1 331 352.8	9.1
$7_{53} \leftarrow 7_{43}$	1 358 170.1	−3.7	1 358 160.6	8.9
$7_{53} \leftarrow 6_{43}$	1 381 903.5	−3.5	1 381 260.5	9.1
$7_{70} \leftarrow 8_{80}$	1 330 762.6	24.7		
$7_{70} \leftarrow 6_{60}$	1 382 127.7	25.1		
$8_{17} \leftarrow 9_{27}$	1 326 560.9	45.1		
$8_{17} \leftarrow 8_{27}$	1 357 126.2	43.8		
$8_{17} \leftarrow 7_{07}$	1 384 311.2	43.7		
$8_{35} \leftarrow 9_{45}$	1 327 576.1	−186.7	1 328 240.2	−17.0
$8_{35} \leftarrow 8_{45}$	1 358 115.8	−186.5	1 358 160.6	−17.0
$8_{35} \leftarrow 7_{25}$	1 385 278.6	−186.6	1 384 785.7	−16.3
$8_{36} \leftarrow 9_{46}$	1 327 188.1	−5.8	1 327 638.4	−40.2
$8_{36} \leftarrow 8_{26}$	1 357 740.1	−7.3	1 357 592.0	−39.7
$8_{36} \leftarrow 7_{26}$	1 384 914.4	−7.4		
$8_{53} \leftarrow 9_{63}$	1 328 922.0	216.7		
$8_{53} \leftarrow 7_{43}$	1 386 492.5	217.9		
$8_{54} \leftarrow 9_{64}$	1 328 323.2	89.2	1 328 722.8	−25.3
$8_{54} \leftarrow 8_{44}$	1 358 850.2	91.0	1 358 642.0	−25.7
$8_{54} \leftarrow 7_{44}$	1 385 996.6	89.9	1 385 210.6	−24.9
$8_{71} \leftarrow 9_{81}$	1 329 603.6	−4.6		
$8_{71} \leftarrow 7_{61}$	1 386 995.1	−4.6		
$8_{72} \leftarrow 9_{82}$	1 328 537.5	−18.3		
$8_{72} \leftarrow 7_{62}$	1 386 366.5	−17.0		
$9_{18} \leftarrow 9_{28}$	1 357 475.5	52.4		
$9_{18} \leftarrow 8_{08}$	1 388 055.7	52.8		
$9_{19} \leftarrow 10_{29}$	1 322 378.3	−181.5		
$9_{19} \leftarrow 9_{09}$	1 356 352.1	−181.2		
$9_{36} \leftarrow 10_{46}$	1 324 877.7	−31.5		
$9_{36} \leftarrow 9_{46}$	1 358 803.7	−32.3		
$9_{36} \leftarrow 8_{26}$	1 389 357.0	−32.6		
$9_{37} \leftarrow 10_{47}$	1 324 244.9	−0.2		
$9_{37} \leftarrow 9_{27}$	1 358 184.8	−2.0		
$9_{37} \leftarrow 8_{27}$	1 388 751.9	−2.5		
$9_{54} \leftarrow 10_{64}$	1 325 888.8	−62.6		
$9_{54} \leftarrow 9_{64}$			1 359 791.0	−15.5
$9_{54} \leftarrow 8_{44}$	1 390 292.4	−62.3	1 389 710.3	−15.8
$9_{55} \leftarrow 10_{65}$	1 325 401.1	−68.5	1 326 179.0	43.8
$9_{55} \leftarrow 9_{45}$	1 359 310.4	−69.3	1 359 395.4	43.7
$9_{55} \leftarrow 8_{45}$			1 389 315.8	43.7
$10_{19} \leftarrow 10_{29}$	1 357 836.5	52.0		
$10_{19} \leftarrow 9_{09}$	1 391 810.1	52.2		
$10_{110} \leftarrow 11_{210}$	1 319 260.6	−162.1		
$10_{110} \leftarrow 10_{010}$	1 356 627.1	−161.9		
$10_{37} \leftarrow 11_{47}$	1 322 048.2	−30.1		
$10_{37} \leftarrow 10_{47}$	1 359 359.8	−29.8		
$10_{37} \leftarrow 9_{27}$	1 393 300.8	−31.0		
$11_{110} \leftarrow 12_{210}$	1 317 478.8	46.6		
$11_{110} \leftarrow 11_{210}$	1 358 210.2	43.6		
$12_{111} \leftarrow 12_{211}$	1 358 600.7	31.1		
$13_{112} \leftarrow 13_{212}$	1 359 011.3	18.1		
$14_{113} \leftarrow 14_{213}$	1 359 445.2	7.6		
$15_{114} \leftarrow 15_{214}$	1 359 903.8	1.1		

TABLE IV. Molecular constants (MHz) for out-of-plane bend of Ar_2HCl.

	$Ar_2H^{35}Cl$	$Ar_2H^{37}Cl$
ν_0	1 355 140.(31.0)	1 355 130.(16.0)
B_x	1 774.(2.0)	1 767.3(1.9)
B_y	1 752.(2.0)	1 679.9(1.3)
B_z	854.6(6)	835.1(7)
D_J	0.06(2)	−0.031 8(7)
D_{JK}	−0.12(5)	−0.039 33(fixed)
D_K	−0.07(3)	0.017 83(fixed)
d_1	0.002 479(fixed)	0.002 927(fixed)
d_2	−0.000 406 6(fixed)	−0.000 456(fixed)
rms error	77.3	21.0

DISCUSSION

Coriolis coupling: General considerations

It may be seen from Table IV that the rms errors from the rotational fits for the out-of-plane bend of Ar_2HCl are substantially larger than would be expected from the experimental uncertainties. This effect is the signature of a strong heterogeneous perturbation, which is most likely due to a Coriolis interaction. In addition, the in-plane and Σ bends are also *expected* to interact via a Coriolis mechanism, although the perturbation is not apparent simply from the residuals resulting from the zero-order rotational fit. We therefore turn to a general discussion of the possible and observed effects of Coriolis coupling in the Ar_2HCl system.

The standard vibration–rotation Hamiltonian used for the fitting of spectra usually neglects the Coriolis cross terms in the full Hamiltonian because such effects are often too small to be determined from experimental data. Although it is possible to treat these effects perturbatively, it is often desirable, especially in the case of fitting to high resolution data and/or strong mixing between states, to explicitly form the full Hamiltonian matrix and diagonalize to obtain energies. The exact form of the Coriolis operator depends on the form of the Hamiltonian used—which in turn is often determined by the most appropriate basis set—but it can be expressed generally as βJ_i, where $i=a, b, c$ (corresponding to the principal axes) and β is a constant. The molecule-fixed axes for Ar_2HCl (Ref. 17) correspond to the principal axes in the following manner for the states of relevance: $x \leftrightarrow a$, $y \leftrightarrow b$, and $z \leftrightarrow c$. In the case of Ar_2HCl, Cooper and Hutson[20] have used a diatom–diatom Hamiltonian, which results in two Coriolis operators: $\mathbf{J}\cdot\mathbf{j}_{Ar-Ar}$ and $\mathbf{J}\cdot\mathbf{j}_{HCl}$. Because $\mathbf{j}_{HCl}$ and especially $\mathbf{j}_{Ar-Ar}$ are only approximate quantum numbers, essentially all states can couple through these operators. In order to determine the appropriate matrix element for any two interaction Ar_2HCl vibrational states, the transformation properties of J_i in the molecular symmetry group $C_{2v}(M)$ must be considered. Because it can be shown that the J_i transform the same as the rotations,[28] reference to the $C_{2v}(M)$ character table reveals J_a, J_b, and J_c transform as A_2, B_1, and B_2, respectively. Therefore, in order to ensure a totally symmetric direct product ($\Gamma_1 \times \Gamma_{Coriolis} \times \Gamma_2 = A_1$), the direct product of the two interacting states ($\Gamma_1 \times \Gamma_2 = \Gamma_{Coriolis}$) indicates the nonvanishing βJ_i.[28] The symmetries of the 10-lowest-lying vibrational states of Ar_2HCl, the nonvanishing Coriolis interactions, and the associated matrix elements (calculated in the oblate symmetric top basis) are presented in Table VI.

TABLE V. Nuclear quadrupole coupling constants and angular expectation values.

	Out-of-plane bend		In-plane-bend	
	$Ar_2H^{35}Cl$	$Ar_2H^{37}Cl$	$Ar_2H^{35}Cl$	$Ar_2H^{37}Cl$
χ_{xx}(MHz)	1.72(15)	0.9(5)	0.0(2)	0.0(2)
χ_{yy}(MHz)	14.08(15)	11.5(5)	−17.2(2)	−13.2(2)
χ_{zz} (MHz)	−15.81(6)	−12.1(2)	17.29(7)	13.3(2)
$\langle P_2(\cos\theta)\rangle$	−0.025(2)	−0.017(9)	0.000(3)	0.000(4)
$\langle\Delta(\theta,\phi)\rangle$	−0.295(2)	−0.309(7)	0.340(3)	0.331(5)

Coriolis coupling: The in-plane and Σ bends

The in-plane and Σ bends[16] are coupled by a *c*-type Coriolis interaction, although the coupling is apparently relatively weak since both bands can be fit with good residuals to the zero-order rotational Hamiltonian parameters. An explicit deperturbation was attempted, using the appropriate form of the matrix element from Table VI, but the multiplying coefficient β could not be determined from the data. Nevertheless, even in the limit of weak coupling, the rotational constants can be substantially affected by such an interaction by as much as a few percent. Because the calculations of Cooper and Hutson yield *structural* rotational constants,[20] it is desirable to recover the structural contributions to the experimental rotational constants (which also include any dynamical effects) in order to make the comparison between theory and experiment.

The $\mathbf{J}\cdot\mathbf{j}_{HCl}$ contribution to the Coriolis coupling constant β can be estimated in the limit of free internal rotation of the HCl monomer (characterized by the angular momentum quantum number $\mathbf{j}_{HCl}$). At this point, it is not possible to reasonably estimate the magnitude of the $\mathbf{J}\cdot\mathbf{j}_{Ar-Ar}$ coupling, therefore, it is arbitrarily set to zero (although there is no real justification for this choice). Estimating β from the $\mathbf{J}\cdot\mathbf{j}_{HCl}$ interaction alone yields $\beta = B_i[2j_{HCl}(j_{HCl}+1)]^{1/2}$. For the particular case of coupling under consideration here, B_i was chosen to be the approximate *structural* rotational constant along the *c* axis (B_z). Since the Ar_2HCl bending states of interest correlate to the $j=1$ rotational state of the HCl monomer, β is simple two times the rotational constant. In direct fits to experimental data for the ArHCl system, the coupling constant between the Σ and Π bends (to which the in- and out-of-plane bends of Ar_2HCl correlate) has been determined to be 2833 MHz or 1.6 times the rotational constant.[29] The deviation of β from $2B$ results from the breakdown of $\mathbf{j}_{HCl}$ as a rigorously good quantum number, which is a consequence of the anisotropic potential. In an attempt to remove the effects of Coriolis coupling from the experimental rotational constants, we have refit the data with

TABLE VI. Symmetries of relevant vibrational states and Coriolis coupling matrix elements.

Symmetries		Coriolis types and matrix elements	
State[a]	Γ	$\Gamma_1\times\Gamma_2$	Matrix element[b]
ground state	A_1	$A_2(a$ type)	$\beta[J(J+1)-K(K\pm1)]^{1/2}\Delta K',K\pm1$
wagging stretch	A_1	$B_1(b$ type)	$\mp\beta[J(J+1)-K(K\pm1)^{1/2}\delta K',K\pm1$
χ bend	B_2	$B_2(c$ type)	$\beta K\delta_{K',K}$
breathing stretch	A_1		
in-plane bend	B_2		
parallel bend	A_1		
out-of-plane bend	B_1		
wag. stretch ($v=2$)	A_1		
χ bend+wag. stretch	B_2		
χ bend ($v=2$)	A_1		

[a]States listed in estimated ascending energy order.
[b]Matrix elements calculated in oblate symmetric top basis.

assumed values for β [and using a structural value of $B_z(s)$ $=850$ MHz]. The results for the in-plane bend in Table II and the parameters reported for the Σ bend in Ref. 16 then correspond to an assumed value of $\beta=0$. Fits for assumed values for β of $2B_z$ (free rotor value), $1.6B_z$ (ArHCl value), and $1.3B_z$ (an educated guess for the more anisotropicAr_2HCl) were performed and the results are contained in Table VII. Because the B_x and B_y rotational constants did not vary with different assumed values for β, only the values for B_z are reported. Although the structural rotational constants calculated by Cooper and Hutson are not in absolute quantitative agreement with experiment (Table VIII),[20] it is interesting to note that the calculated *difference* between the in-plane and Σ bend B_z constants (21 MHz) is in much better agreement with the experimental difference for an assumed value of $\beta=1.3B_z$ (22 MHz) than for any of the other assumed values of beta. In addition, in order to appreciate the small magnitude of this interaction, the sum-of-squares wave-function amplitudes recovered from the matrix diagonalization for three rotational levels of the in-plane bend are also reported in Table VII. The small degree of mixing in the $J=5$ rotational level is particularly significant since the nuclear hyperfine quadrupole coupling constants for the in-plane and Σ bends were fitted from similar low-J rovibrational transitions. Therefore, the fact that the hyperfine structure could be accurately fitted without explicitly treating the Coriolis interaction is consistent with the notion that the perturbation is quite weak. Nevertheless, we again note that even this weak perturbation causes changes of $\sim2\%$ in the effective rotational constants determined from a fit of the data to a pure rotational Hamiltonian ($\beta=0$). For the purposes of comparing experimental and theoretical rotational constants in an effort to determine possible three-body effects in Ar_2–HCl, neglecting Coriolis effects to the rotational constants that result in deviations as much as 2% from the corresponding "structural" values is an unacceptable approximation.

TABLE VII. Results of in-plane and parallel bend Coriolis analysis.

	$\beta=2B_z(s)$	$\beta=1.6B_z(s)$	$\beta=1.3B_z$ s(s)	$\beta=0$
in-plane bend B_z (MHz)	867.44	852.72	843.85	826.70
parallel bend B_z (MHz)	842.24	856.96	865.83	883.04
In-plane bend contribution to the square modulus of the wave function for a number of individual rotational states				
$\lvert\psi_{\text{in-plane}}(5_{15})\rvert^2$	0.98	0.99	0.99	1.00
$\lvert\psi_{\text{in-plane}}(10_{110})\rvert^2$	0.95	0.97	0.98	1.00
$\lvert\psi_{\text{in-plane}}(15_{115})\rvert^2$	0.91	0.94	0.96	1.00

Coriolis coupling: The out-of-plane bend

The out-of-plane bend of Ar_2HCl appears to be much more strongly perturbed, as is evidenced by the large residuals resulting from the zero-order rotational fit. In fact, the rms error is more than two orders of magnitude larger than the experimental uncertainties. In addition, although the uncertainties in the rotational constants reflect the poor fit, it should be noted that the results for the Ar_2H ^{37}Cl isotope cannot be obtained by simply mass scaling the Ar_2H ^{35}Cl results, indicating that the fitted constants may be less reliable than the stated uncertainties reveal.

Unfortunately, the perturbing state is almost definitely one that carries little transition intensity of its own (a "dark" state). The calculations of Cooper and Hutson indicate that the first overtone of the "wagging stretch" (see Cooper and Hutson[20] for an explanation of the heavy-atom vibrational modes) is the most likely candidate for the identity of the dark state.[30] In fact, all possible perturbing states are heavy-atom vibrations whose motions do not result in an appreciable change in the dipole moment of the complex and are therefore "dark." Although there are many unassigned lines in the spectral region around the out-of-plane bend, it was not possible to definitively assign any of these lines to a possible perturbing state, and therefore it is not currently possible to perform a rigorous deperturbation of the spectra. In addition, it is difficult to provide an estimate for β, since the coupling of the end-over-end rotation to these motions is *not* easily represented in the otherwise-convenient free-rotor basis. However, it is worth noting that the β parameter for the Π bend–stretch

TABLE VIII. Comparison of experimental and theoretical results for $Ar_2H\,^{35}Cl$.

	Observed (1σ)	Calc. 1[a]	Calc. 2[b]	Calc. 3[c]
		Ground state[d]		
B_x(MHz)	1733.8560(4)	···	1757.19	1756.99
B_y(MHz)	1667.921 40(4)	1702.4	1671.10	1668.24
B_z(MHz)	844.444 87(16)	857.6	849.53	848.73
$\langle P_2(\cos\theta)\rangle$	0.4165(4)	0.4540	0.4472	0.4429
$\langle\Delta(\theta,\phi)\rangle$	0.0313(2)	0.02179	0.0222	0.0255
		In-plane bend[e]		
$\nu_0(\mathrm{cm}^{-1})$	37.195 426(10)	40.315	39.587	39.190
B_x(MHz)	1683.61(2)	···	1744.23	1744.98
B_y(MHz)	1682.42(2)	1730.8	1694.27	1686.04
B_z(MHz)	826.702(9)	864.8	851.25	849.22
$\langle P_2(\cos\theta)\rangle$	0.000(3)	−0.0330	−0.0191	−0.0031
$\langle\Delta(\theta,\phi)\rangle$	0.340(3)	0.3673	0.3531	0.3441
		Σ bend[f]		
$\nu_0(\mathrm{cm}^{-1})$	39.554 709(10)	42.589	40.734	41.325
B_x(MHz)	1733.70(4)	···	1753.23	1753.72
B_y(MHz)	1720.89(3)	1793.4	1758.94	1766.59
B_z(MHz)	883.040(13)	879.2	868.55	870.47
$\langle P_2(\cos\theta)\rangle$	0.291(3)	0.2943	0.2772	0.2752
$\langle\Delta(\theta,\phi)\rangle$	0.062(7)	0.04296	0.0474	0.0591
		Out-of-plane bend[g]		
$\nu_0(\mathrm{cm}^{-1})$	45.2026(10)	47.236	46.686	46.542
B_x(MHz)	1774.0(2.0)[h]	···	1750.15	1749.94
B_y(MHz)	1752.0(2.0)[h]	1740.8	1706.72	1705.52
B_z(MHz)	854.6(6)[h]	867.1	856.59	856.21
$\langle P_2(\cos\theta)\rangle$	−0.025(2)	−0.0030	−0.0140	−0.0224
$\langle\Delta(\theta,\phi)\rangle$	−0.295(2)	−0.3098	−0.3146	−0.3197

[a]Calc. 1 refers to the dynamically approximate clamped-Ar_2 calculations on the H6(3)+HFD-C pairwise-additive surface (Ref. 15).
[b]Calc. 2 refers to the full five-dimensional dynamical calculation on the H6(3)+HFD-C pairwise-additive surface (Ref. 20).
[c]Calc. 3 refers to the full five-dimensional dynamical calculation on the H6(4,3,0)+HFD-C pairwise additive surface (Ref. 20).
[d]References 16 and 24.
[e]Reference 17 and this work.
[f]Reference 16.
[g]This work.
[h]See text for discussion of reliability of these fitted constants.

interaction in ArHCl was experimentally determined to be about one-third of the value determined for the Σ–Π bend interaction.[29] Because of the smaller coupling coefficient, one would expect a bend–stretch interaction to be more *localized* (more dependent on near resonance) than a similar bend–bend interaction.

It is of considerable interest to determine the probable energy separation of the two interacting states for the purpose of roughly locating the position of the "dark" state. By using features of the spectra to determine where the two interacting states "cross" (become resonant) one can obtain a qualitative estimate of the desired energy difference. Clearly, large residuals in the zero-order rotational fit indicate states which are more nearly resonant than states with smaller residuals. In addition, the observed nuclear quadrupole hyperfine structures are also determined by a linear combination of the pure "bright" and "dark" state hyperfine contributions. Consequently, large rotational residuals should correlate with large hyperfine residuals. It should be noted that the *relative* measured accuracy for the hyperfine energies (1 to 10^2) is much less than the *relative* measured accuracy for rotational energies (10^4 to 10^5). Therefore, the hyperfine structure is not as sensitive to perturbations as are the rotational energies.

Unfortunately, only four transitions with exceptionally large rotational residuals (>60 MHz) have fully resolved (and therefore more accurately measured) hyperfine structure. By reference to Table I, it may be seen that the transitions which involve the 6_{16}, 7_{17}, 9_{19}, and 10_{110} upper state levels possess very large rotational residuals and it is these transitions for which fully resolved hyperfine structure has been measured. It is also of interest to note that the 6_{16} and 7_{17} levels are characterized by large *positive* residuals while the 9_{19} and 10_{110} levels are characterized by large *negative* residuals. This is suggestive of a "crossing" occurring around the 8_{18} level, which has thus far eluded assignment. The nuclear quadrupole structure also shows evidence for strong mixing; these transitions are the only fully resolved hyperfine spectra which, upon inclusion in the hyperfine fit, did not yield residuals consistent with expected experimental uncertainties. In an attempt to further quantify the correlation between the rotational and hyperfine residuals, the upper state hyperfine coupling constants associated with these transitions were assumed to be the result of the following linear combination:

$$\chi_{ii}(\text{observed}) = c^2\chi_{ii}(\text{dark state}) + (1-c^2)\chi_{ii}(\text{out-of-plane bend}). \quad (3)$$

The χ_{ii} for the out-of-plane bend were fixed at the experimentally determined values and the χ_{ii} for the dark state were assumed to be the same as for the ground state (a good approximation for the heavy-atom vibrational states in the limit of weak potential coupling to the HCl bending states). The hyperfine structure for each transition was subsequently fit, with c as the variable parameter. The determined c coefficients did indeed correlate with the rotational residuals, yielding values (rotational residuals in parentheses) of 0.27 (98 MHz), 0.55 (248 MHz), 0.36 (−181 MHz), and 0.34 (−162 MHz) for the 6_{16}, 7_{17}, 9_{19}, and 10_{110} levels, respectively. As a caveat, it should be noted that the quality of the fit was not sensitive to the χ_{ii} values assumed for the dark state. However, this information is strong support for a fairly localized perturbation that is near resonant around the 8_{18} rotational level of the out-of-plane bend. Because the "crossing" occurs at a relatively low total rotational energy (about 4 cm^{-1}), it is likely that the separation of the two interacting vibrational states is 1 cm^{-1} or less.

Coriolis coupling: General conclusions

From the arguments presented above, it is apparent that Coriolis mixing in the Ar_2HCl system can lead to substantial effects in the spectra through a subtle interaction (the in-plane-bend–Σ-bend interaction) or more obviously, through a strong perturbation (the out-of-plane–

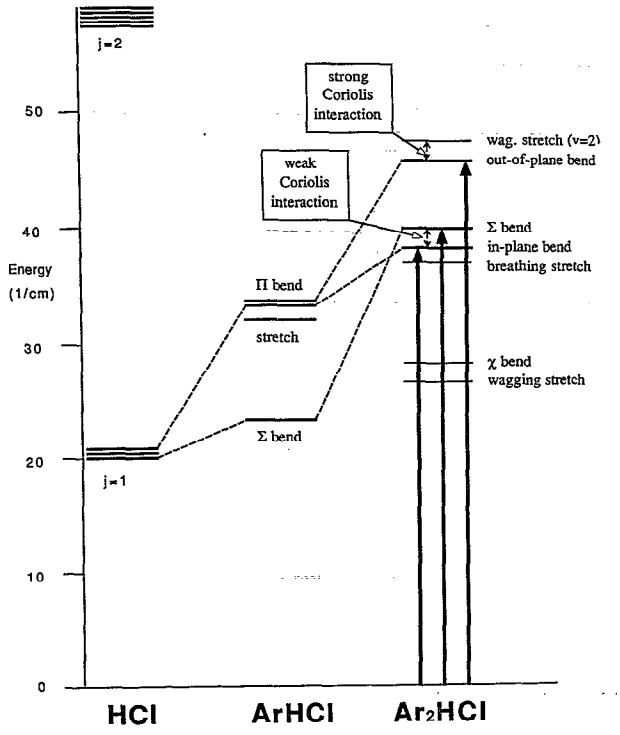

FIG. 2. Energy level correlation diagram for the Ar_nHCl ($n=0,1,2$) systems. Measured far infrared transitions for Ar_2HCl are denoted by solid arrows. States whose energies have been experimentally determined are represented by thick lines and calculated states (thin lines) are from the results of Cooper and Hutson (Ref. 20).

$v=2$ wagging stretch interaction). Although these instances should become more ubiquitous as the cluster size increases (due to an increase in the density of states), these interactions have been shown to have important effects on the spectra of all four prototypical binary systems mentioned in the introduction (ArHCl, ArHF, ArH_2O, and $ArNH_3$).[7–10] Weak Coriolis interactions are particularly troublesome since it is often not possible to detect the existence of such coupling from fits to a purely rotational Hamiltonian, although the effects on the rotational constants can still be substantial. Accurate vibrational calculations for Ar_2HCl have made an approximate understanding of these effects possible, although full rovibrational calculations will be needed to fully account for these interactions. We emphasize that similar considerations should be expected to be important for similar and larger systems and that these effects will likely *often* compromise a "structural" interpretation of experimental rotational constants.

Comparison of experiment and theory

Since all three Ar_2HCl bending vibrations that correlate to the $j=1$ internal rotational state of the HCl monomer (see Fig. 2) have now been measured, the experimental data set is sufficient to warrant a meaningful comparison with theoretical results. For the purposes of exploring the capabilities and limitations of various theoretical efforts, we have included comparisons with three different pairwise-additive calculations (Table VIII). The three-dimensional (Ar_2 clamped) dynamical calculations of Hutson, Beswick, and Halberstadt[15] using the H6(3) potential[31] are expected to be the least accurate results because of the dynamically approximate nature of the method and the use of the now-superseded H6(3) ArHCl pair potential. Also included for comparison are the recent calculations of Cooper and Hutson[20] which fully treat the five-dimensional dynamical problem. They have used a variational method with both the H6(3) and the more reliable H6(4,3,0) ArHCl pair potentials in order to determine the sensitivity of the molecular parameters to the ArHCl pair potential. Therefore, comparison between columns 2 and 3 in Table VIII indicate separately the effects of the dynamical approximation of Hutson, Beswick, and Halberstadt [for both calculations use the H6(3) ArHCl pair potential] and comparison between columns 3 and 4 indicate separately the effects of the different pair potentials on the molecular parameters (for both calculations are dynamically rigorous).

It may be seen that there are fairly substantial differences between the dynamically approximate and the full five-dimensional calculation, thus demonstrating the necessity of the computationally expensive calculation. In our previous analysis of the in-plane bend,[17] we concluded that the experimental rotational constants indicated substantial potential coupling between the Ar_2 coordinates and the HCl bending motions and that for this reason more rigorous dynamical calculations were needed. The reassignment of the in-plane bend and the resulting molecular constants in this work does not compromise the logic of those conclusions, which were based on changes in the experimental rotational constants on the order of a few percent. However, the full dynamical calculations actually reveal very small *potential* mixing of these states.[20] We have shown in this work that even weak Coriolis perturbations can lead to significant changes in the experimental rotational constants and that "structural" conclusions based on small changes in the experimental rotational constants are, in fact, extremely tenuous. Indeed, inspection of the experimental and calculated rotational constants for all three excited bending states reveals some very substantial discrepancies, indicating the probable effects of Coriolis coupling. In order to allow comparison between experiment and theory for these very valuable parameters, it will be necessary to explicitly treat these Coriolis effect effects in future calculations.

The agreement between calculated and observed band origins and angular expectation values is qualitatively good. However, in the instance of agreement between the measured and calculated band origins, it should be noted that experimental uncertainties are on the order of less than 0.001 cm^{-1} and the level of convergence for these calculated quantities[20] is about 0.01 cm^{-1}, whereas the discrepancies *between* the measured and calculated values are larger than 1 cm^{-1}. Therefore, it must be concluded that the pairwise-additive potential energy surface is not sufficiently accurate to obtain agreement with experiment. The comparison between calculations using the two differ-

ent ArHCl potentials provides some measure of the possible discrepancies introduced by slight inaccuracies in the pair potentials. Although the differences resulting from the two calculations are non-negligible, it may be noted that the discrepancies between the two theoretical values are substantially less than the discrepancy between experimental and theoretical values. In addition, the results from the more accurate potential do not necessarily correspond with better agreement with experiment. Therefore, it may be concluded that potential inadequacies in the ArHCl pair potential *cannot* be entirely responsible for the theoretical–experimental inconsistencies. However, the results of Cooper and Hutson[20] indicate that the effects of three-body forces can indeed be of the same magnitude as the current disagreement between experiment and theory and that it should be possible to directly determine these forces from the spectra reported in this work. Such efforts are in progress.

ACKNOWLEDGMENTS

The authors wish to thank Jeremy Hutson and Adam Cooper for providing the results of preliminary calculations and for helpful discussions throughout the course of this work. This work was supported by the National Science Foundation (Grant No. CHE-9123335). M.J.E. thanks the University of California for a graduate fellowship.

[1] G. Chalasinski, S. M. Cybulski, M. M. Szczesniak, and S. Scheiner, J. Chem. Phys. **91**, 7048 (1989).
[2] M. M. Szczesniak, R. Kendall, and G. Chalasinski, J. Chem. Phys. **95**, 5169 (1991).
[3] G. Chalasinski, M. M. Szczesniak, and S. M. Cybulski, J. Chem. Phys. **92**, 2481 (1990).
[4] G. Chalasinski, M. M. Szczesniak, and S. Scheiner, J. Chem. Phys. **94**, 2807 (1991).
[5] G. Chalasinski, M. M. Szczesniak, and B. Kukawska-Tarnawska, J. Chem. Phys. **94**, 6677 (1991).
[6] A. R. Cooper, S. Jain, and J. M. Hutson, J. Chem. Phys. **98**, 2160 (1993).
[7] J. M. Hutson, J. Phys. Chem. **96**, 4237 (1992).
[8] J. M. Hutson, J. Chem. Phys. **96**, 6752 (1992).
[9] R. C. Cohen and R. J. Saykally, J. Phys. Chem. **94**, 7991 (1990); J. Chem. Phys. (submitted).
[10] C. A. Schmuttenmaer, J. G. Loeser, and R. J. Saykally (unpublished).
[11] S. Novick, K. Leopold, and W. Klemperer, in *Atomic and Molecular Clusters,* edited by E. Bernstein (Elsevier, Amsterdam, 1990).
[12] R. C. Cohen and R. J. Saykally, J. Phys. Chem. **96**, 1024 (1992).
[13] D. J. Nesbitt, Chem. Rev. **88**, 843 (1988).
[14] M. J. Elrod, B. C. Host, D. W. Steyert, and R. J. Saykally, Mol. Phys. (in press).
[15] J. M. Hutson, J. A. Beswick, and N. Halberstadt, J. Chem. Phys. **90**, 1337 (1989).
[16] M. J. Elrod, D. W. Steyert, and R. J. Saykally, J. Chem. Phys. **94**, 58 (1991).
[17] M. J. Elrod, D. W. Steyert, and R. J. Saykally, J. Chem. Phys. **95**, 3182 (1991).
[18] A. McIlroy, R. Lascola, C. M. Lovejoy, and D. J. Nesbitt, J. Phys. Chem. **95**, 2636 (1991).
[19] A. McIlroy and D. J. Nesbitt, J. Chem. Phys. **97**, 6044 (1992).
[20] A. R. Cooper and J. M. Hutson, J. Chem. Phys. **98**, 5337 (1993), preceding paper.
[21] G. A. Blake, K. B. Laughlin, K. L. Busarow, R. C. Cohen, D. Gwo, C. A. Schmuttenmaer, D. W. Steyert, and R. J. Saykally, Rev. Sci. Instrum. **62**, 1701 (1991).
[22] G. A. Blake, K. B. Laughlin, K. L. Busarow, R. C. Cohen, D. Gwo, C. A. Schmuttenmaer, D. W. Steyert, and R. J. Saykally, Rev. Sci. Instrum. **62**, 1693 (1991).
[23] I. G. Nolt, J. V. Radostitz, G. DiLonardo, K. M. Evenson, D. A. Jennings, K. R. Leopold, M. D. Vanek, L. R. Zink, A. Hinz, and K. V. Chance, J. Mol. Spectrosc. **125**, 274 (1987).
[24] T. D. Klots, C. Chuang, R. S. Ruoff, T. Emilsson, and H. S. Gutowsky, J. Chem. Phys. **86**, 5315 (1987).
[25] T. D. Klots and H. S. Gutowsky, J. Chem. Phys. **91**, 63 (1989).
[26] J. K. G. Watson, J. Chem. Phys. **46**, 1935 (1967).
[27] H. P. Benz, A. Bauder, and Hs. H. Gunthard, J. Mol. Spectrosc. **21**, 156 (1966).
[28] P. R. Bunker, *Molecular Symmetry and Spectroscopy* (Academic, New York, 1979).
[29] S. W. Reeve, M. A. Dvorak, D. W. Firth, and K. R. Leopold, Chem. Phys. Lett. **181**, 259 (1991).
[30] A. R. Cooper and J. M. Hutson (private communication).
[31] J. M. Hutson, J. Chem. Phys. **89**, 4550 (1988).